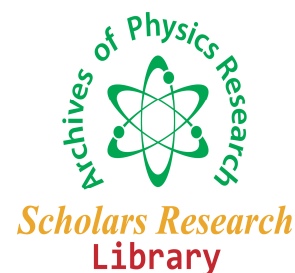




Scholars Research Library

Archives of Physics Research, 2010: 1 (1) 112-118
(<http://scholarsresearchlibrary.com/archive.html>)



Structural, Dielectric and Magnetic Properties of Nanocrystalline Ni-Zn Ferrites

P. U. Mahamuni and B. K. Chougule*

Soft Ferrite Materials Laboratory, Department of Physics, Shivaji University, Kolhapur, India

Abstract

Nanoferrites are more superior to conventional coarse grain ferrite materials and have been the focus of recent studies. A series of nanocrystalline Ni-Zn ferrites with the composition $\text{Ni}_x\text{Zn}_{1-x}\text{Fe}_2\text{O}_4$ (where $x = 0.2, 0.4, 0.6, 0.8$) were prepared by sucrose method. The samples were sintered at 900°C for 12h to densify them properly. The samples were characterized by XRD, TEM and IR spectroscopy. The dielectric constant ϵ' and dielectric loss tangent ($\tan \delta$) were measured as a function of frequency and the magnetic properties were measured by using high field hysteresis loop tracer.

Key words: Sucrose method, nanocrystalline ferrites, IR spectra, magnetic properties.

Introduction

Ferrites are a commercially important family of materials. They show high electrical resistivity, low losses and high permeability at higher frequencies. Due to small particle size nanostructured ferrites possess possibility to develop high density magnetic storage media used in computer and electronic industries [1-4].

Ni-Zn ferrites are ferrimagnetic materials that have large number of applications in telecommunication and entertainment electronics. They possess high electrical resistivity making them suitable for applications at higher frequencies. They exhibit high value of saturation magnetization, magnetic permeability, Curie temperature and dielectric constant [5]. These advantageous characteristics lend them useful as magnetic recording heads [6].

Properties of ferrites are microstructure dependent which is very sensitive to the manufacturing process [7, 8, and 9]. Remarkable improvements in the properties of ferrite nanoparticles make them useful in electronics, bioprocessing, magnetic resonance image enhancement and ferrofluids [10-13].

Several methods of synthesis of nanocrystalline ferrites such as sol gel, co-precipitation, oxidation and reverse mischell technique have been proposed in recent years. The sucrose method is one of the solution based chemical synthesis methods for preparation of fine grained powders. The process improves purity, homogeneity and minimizes agglomeration.

Materials and Methods

2. Experimental

2.1 Preparation

Nanocrystalline $\text{Ni}_x\text{Zn}_{1-x}\text{Fe}_2\text{O}_4$ powders were synthesized by sucrose method using metal nitrates of AR grade purity. Initially nickel nitrate, zinc nitrate and iron nitrate were weighed in desired stoichiometric proportions and their solution was prepared in distilled water. To this solution, 10% aqueous solution of PVA and sucrose were mixed and solution was evaporated. Resulting solution was heated at about 200°C to remove NO_2 vapors completely in the form of brown fumes. This gives black, fluffy, voluminous organic based mass, the precursor material. Proper heat treatment to precursor forms nanocrystalline ferrites. The ferrites were then sintered at 900°C for 12 h [14].

2.2 Characterization

X-ray diffractograms of the samples were recorded using X-ray diffractometer (Philips Model PW 3710) using $\text{CuK}\alpha$ radiations ($\lambda = 1.5418 \text{ \AA}$). The transmission electron microscope (TEM model JEOL- 1200 EX) was used to study the microstructure. IR spectra of the samples were obtained by using Perkin Elmer IR spectrometer (Model 783) in the range 350cm^{-1} to 700cm^{-1} in KBr medium. The electrical resistivity was measured by two probe method. The dielectric constant was measured in the frequency range 20 Hz to 1 MHz at room temperature using LCR Meter Bridge (Model HP 4284 A). The samples were painted with silver paste to ensure good electrical contacts. High field hysteresis loop tracer of Magneta was used to measure the saturation magnetization.

Results and discussion

3.1 XRD and IR

Fig.1 shows x-ray diffraction patterns of Ni-Zn ferrite samples. The patterns show the formation of single phase cubic spinel structure. The lattice parameter 'a' increases with increase in Zn content as shown in Table-1.

Table - 1 Data on lattice parameter for nanocrystalline $\text{Ni}_x\text{Zn}_{1-x}\text{Fe}_2\text{O}_4$ samples

Sr. No.	composition (x)	Lattice parameter 'a', \AA
1	0.2	8.416
2	0.4	8.370
3	0.6	8.359
4	0.8	8.351

This can be explained on the basis of relative ionic radii of Fe^{2+} , Zn^{2+} and Ni^{2+} . Zn^{2+} ions have ionic radius of 0.83 \AA and Ni^{2+} , Fe^{2+} have ionic radii 0.74 \AA , 0.65 \AA respectively [2]. Addition of Zn^{2+} causes extension of unit cell dimensions thereby increasing lattice parameter. Fig. 2 shows TEM micrographs of samples. The average particle size ranges from 30 nm to 50 nm.

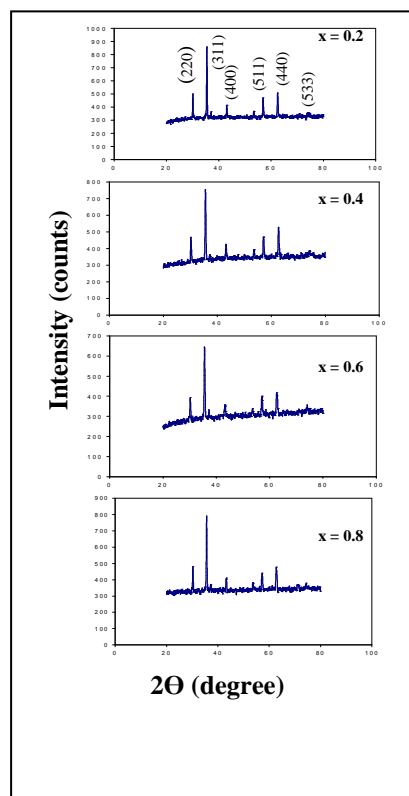


Fig. 1 XRD patterns of nanocrystalline $\text{Ni}_x\text{Zn}_{1-x}\text{Fe}_2\text{O}_4$ ferrite samples

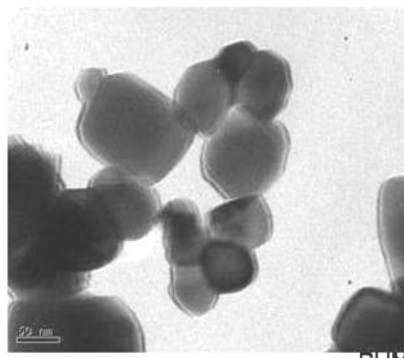


Fig.2 TEM micrograph for nanocrystalline Ni-Zn ferrites samples

Fig.3 shows IR absorption spectra of the samples. The samples show two absorption bands that correspond to vibrations of metal ions on tetrahedral and octahedral sites of the spinel structure respectively. Waldron [15] has attributed the ν_1 band around 600cm^{-1} to the intrinsic vibrations of the tetrahedral group and ν_2 band around 400cm^{-1} to octahedral group. The data is listed in table 2. These bands are mainly dependent on Fe-O distances. The vibrational frequency depends on cation mass, cation-oxygen distance and the bonding force. Higher frequency band is due to stretching vibration and lower frequency band is due to bending vibration. The difference in two band positions is expected because of difference in Fe-O distance according to cation distribution.

Table -2 Data on of IR absorption bands of nanocrystalline $Ni_xZn_{1-x}Fe_2O_4$ samples

Sr. No.	Composition (x)	Frequency ν_1, cm^{-1}	Frequency ν_2, cm^{-1}
1	0.2	572.07	423.36
2	0.4	577.79	417.08
3	0.6	582.91	416.96
4	0.8	586.81	416.97

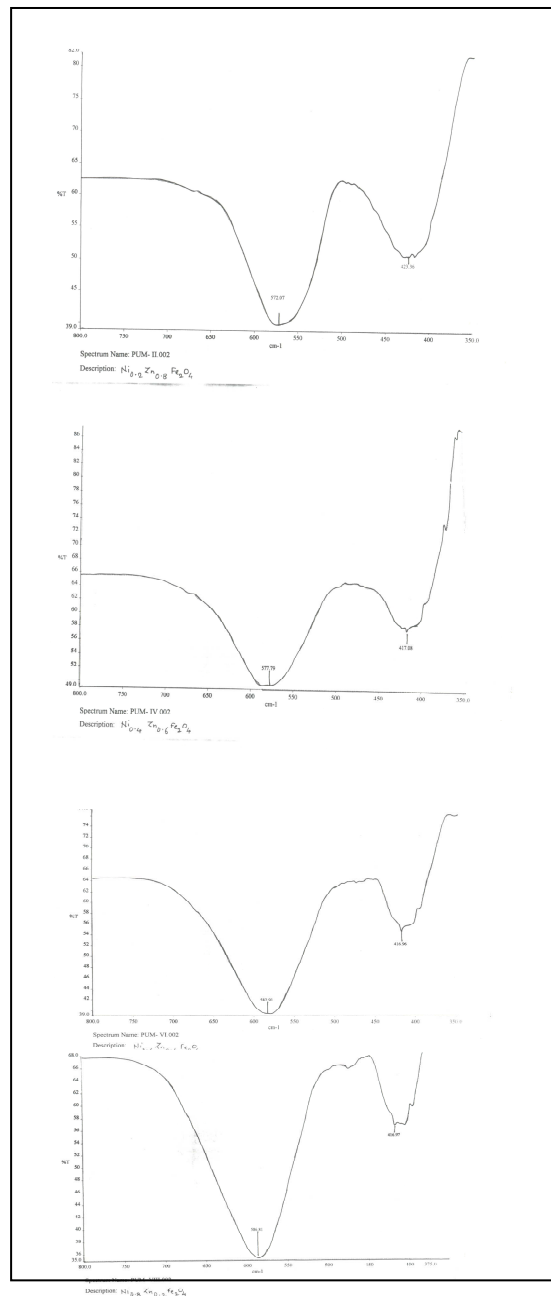


Fig. 3 Position of IR bands in nanocrystalline Ni Zn ferrite

3.2 Dielectric properties

The dielectric constant ϵ' was measured in the frequency range 100 Hz to 1 MHz at room temperature. The dielectric constant was calculated by using the relation,

$$\epsilon' = cd/\epsilon_0 A \quad \dots (1)$$

where c is capacitance of pellet, d is thickness of pellet, A is area of flat surface of pellet, ϵ_0 is permittivity of free space ($\epsilon_0 = 8.85 \times 10^{-12}$ F/m). The variation of dielectric constant ϵ' and loss tangent ($\tan \delta$) with frequency is shown in Fig. 4 and Fig. 5 respectively. The dispersion in dielectric constant and loss tangent is observed in the lower frequency range. The extent of dispersion is affected by Zn content. As Zn content goes on decreasing the dielectric constant increases for all frequencies. The electron exchange between Fe^{2+} and Fe^{3+} results in local displacement of charges in direction of electric field which is responsible for polarization in ferrites. As frequency of externally applied field increases the electronic exchange between Fe^{2+} and Fe^{3+} cannot follow the alternating field decreasing the dielectric constant. The dielectric loss in ferrites results due to electron hopping in lower frequency range.

Fig. 4 Variation of dielectric constant(ϵ') with frequency for nanocrystalline Ni-Zn ferrites

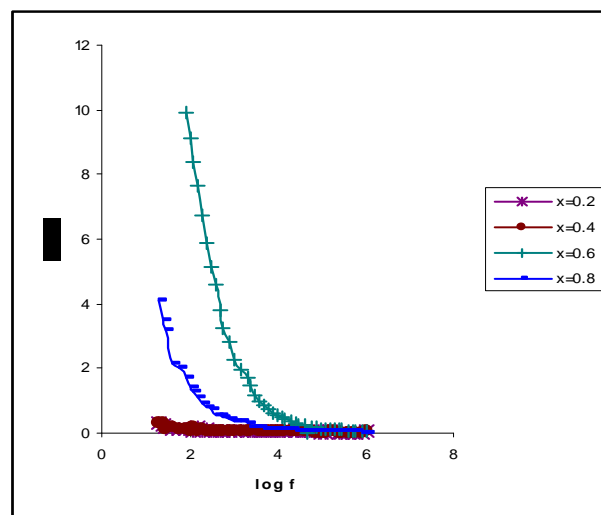
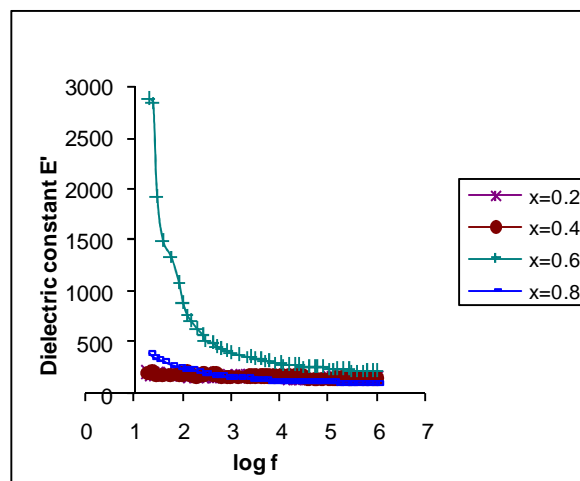


Fig.5 Variation of loss tangent($\tan \delta$) with frequency for nanocrystalline Ni-Zn ferrites



In the higher frequency range the dielectric loss results from response of the dipoles to the field. These dipoles in ferrites are formed due to change of cation valance state as $\text{Ni}^{2+} / \text{Ni}^{3+}$, $\text{Fe}^{2+} / \text{Fe}^{3+}$ during sintering. Relaxation of such dipoles decreases with increasing frequency. And hence dielectric loss decreases at higher frequencies.

3.3 C. Saturation magnetization and magnetic moment

The variation of magnetic moment and saturation magnetization with Zn content is shown Fig. 6 and Fig. 7.

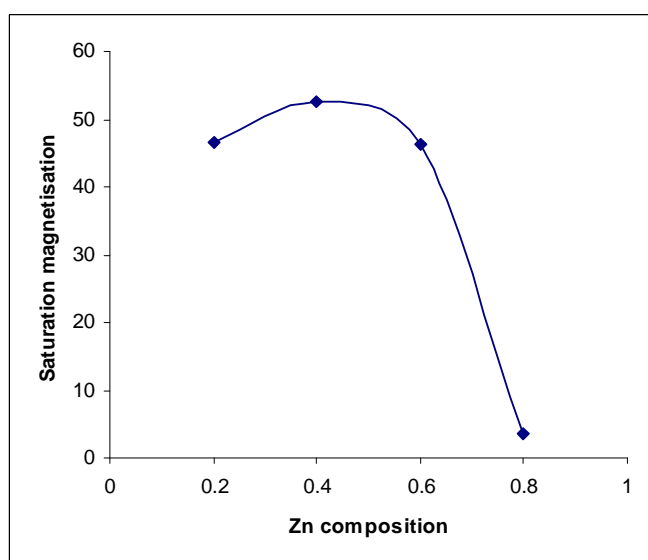


Fig. 6 Variation of magnetic moment with Zn content for nanocrystalline Ni-Zn ferrites

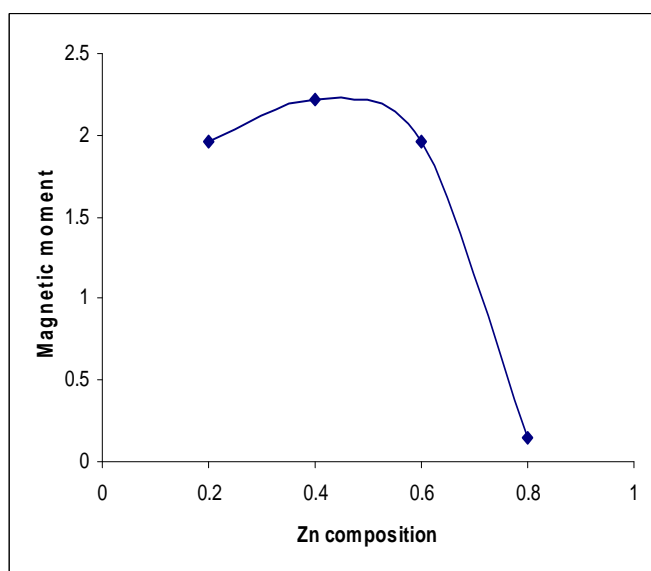


Fig. 7 Variation of saturation magnetization with Zn content for nanocrystalline Ni-Zn ferrites

On the basis of site preference Zn occupies tetrahedral A site while Ni^{2+} and Fe^{3+} occupy octahedral B site. As Zn concentration increases it transfers Fe^{3+} ions from A site to B sites which affects A-B interaction. This results in increase of resultant saturation magnetization up to $x = 0.6$ and then it decreases. Kulkarni *et. al.* [16] have explained initial increase in saturation magnetization with Zn content on the basis of two sublattice model and the decrease on the basis of Yafet Kittle model.

Conclusion

Nanocrystalline single phase Ni-Zn ferrite powders with different compositions were prepared by sucrose method. The x-ray analysis shows formation of single phase cubic spinel structure with an average particle size ranging from 30 nm to 50 nm. The dielectric constant and dielectric loss decrease with frequency of the applied electric field. The magnetic moment and saturation magnetization show remarkable changes due to the addition of Zn.

References

- [1] E. C. Snelling, "Soft ferrites- Properties and Applications" IInd Edition, Butterworths
- [2] J. Smit and H. P. J. Wijn "Ferrites" Eindhoven, Philips Technical Labrary, (1959)
- [3] J. Y. Hsu, W. S. Ko, H. D. Shen, and C.J. Chen, *IEEE Trans. Magn.* 30 (1994) 4875
- [4] S. Ge, Z. zhang, M. zhong Wu, Y. D. Zhang, D. P. Yang, J. I. Budanik and W. A. Hines *Mater. Res. Soc. Symp.* 755 (2003)
- [5] V. Uskokovic, M. Drofenik and I. Ban, *J. Magn. & Magn. Mater.* 284 (2004) 294
- [6] T. Pannaparayil, S. Komarneni, R. Marande, M. Zardrho, *J. Appl. Phys.* 67 (1990) 5509
- [7] A. Dias, *Mater. Res. Bull.* 35 (2000) 1436-1439
- [8] K. Ishino, Y. Narumiga, *Amer. Ceram. Soc. Bull.* 66 (1987) 1469
- [9] M. Popovici, C. Savii, D. Niznansky, J. Subrt, J. Bohacek, D. Becherescu, C. Caizer, C. Enache and C. Ionescu, *J. Optoele. & Mater.* 5 (1) (2003) 251-256
- [10] R. S. Molday and D. Mackenzie, *J. Imm. Methods* 52 (1982) 353
- [11] J. Popplewell and L. Sakhnani, *J. Magn. Magn. Mater.* 149 (1995) 72
- [12] K. Raj. B. Moskowitz and R. Casciari, *J. Magn. & Magn. Mater.* 149 (1995) 174
- [13] C.W. Jung, P. Jacobs, *Magn. Reson. Imaging* 13 (1995) 661
- [14] R. N. Das, *Mat. Lett.* 47 (2001) 344 – 350
- [15] R. D. Waldron, *Phys. Rev.* 99 (1955) 1727
- [16] R. G. Kulkarni and V. G. Panickar, *J. Mater. Sci.* 19 (1984) 890